

The Boundary Layers of an Unsteady Stagnation Points Flow in Carbon Nanotubes

Open
Access

Dhurgham Allaw^{1,*}, Norfifah Bachok^{1,2}, Norihan Md Arifin^{1,2}, Fadzilah Md Ali^{1,2}

¹ Institute for Mathematical Research, Univirsiti Putra Malaysia, 43400 UPM Serdang, Selangor, Malaysia

² Department of Mathematics, Faculty of Science, Universiti Putra Malaysia, 43400 UPM Serdang, Malaysia

ARTICLE INFO

ABSTRACT

Article history:

Received 2 April 2020

Received in revised form 15 July 2020

Accepted 20 July 2020

Available online 3 September 2020

The unsteady stagnation-point boundary layer flow of carbon nanotubes is studied. Single-wall and multi-wall of carbon nanotubes are considered with H_2O as a carrier fluid. The compatible transformations are utilized to change the governing equations of mathematical model which is in the form of partial differential equations (PDE_s) into a set of a non-linear ordinary differential equations (ODE_s). Solution of the problem obtained numerically through a powerful function (*bvp4c*) in MATLAB software. The impact of solid volume fraction and unsteadiness parameters on dimensionless velocity and temperature flow fields along with the magnitude of skin friction coefficient and local Nusselt number are discussed graphically and interpreted physically. The outcome indicates that the dual solutions observed when unsteadiness parameter is negative. Further, single-wall carbon nanotube has higher skin friction, as well as heat transfer rate, compare with multi-wall carbon nanotube at the surface.

Keywords:

Unsteady boundary layer; Carbon
Nanotubes; Stagnation point flow; Dual
solutions

Copyright © 2020 PENERBIT AKADEMIA BARU - All rights reserved

1. Introduction

In the present world of science and technology, the research on nanofluid has gained a remarkable growth due to their extensive applications in all field of science. Choi [1] presented a fascinated concept known as nanofluid which is a homogenous mixture of solid nanoparticles such as alumina, titania, iron, copper and carbon nanotube with carrier fluid such as water, gasoline oil, kerosene oil, ethanol and ethylene. The reason for utilizing solid nanoparticles in carrier fluid is to enhance thermal properties of carrier fluid. Thus, nanofluid has unlimited thermal management characteristic. The new characteristic of nanofluid stimulated a number of researchers to expand the application of nanofluid in differs scope such as automotive industries, nuclear reactors, heat exchangers and biomedicine.

* Corresponding author.

E-mail address: dhurghammohammed09@gmail.com

<https://doi.org/10.37934/arfmts.75.1.1220>

Later, Buongiorno [2] developed a new model by taking into account seven slip mechanisms, two of them are vital in nanofluid namely, Brownian diffusion and thermophoresis. The author found that the properties of nanofluid are different in boundary layer due to temperature gradient and thermophoresis. Tiwari and Das [3] presented a fundamental model that examined thermal properties that are affected by nanoparticle volume fraction. The two models have been used by a large number of researchers over different geometries. Bachok *et al.*, [4] reported the influence of solid volume fraction on stagnation-point flow over stretching/shrinking permeable surface. Das *et al.*, [5] explored numerically the effect of non-linear radiation, homogeneous-heterogeneous reaction and mixed convection parameters on stagnation point nanofluid flow towards a linearly stretching surface. Uddin *et al.*, [6] found out the heat and mass transfer analysis past a moving vertical surface.

The non-Newtonian fluid namely Jeffery fluid debated by Ahmad and Ishak [7] the authors examined the effects of mixed convection and MHD parameters through a stretching vertical surface immersed in porous medium. Stability analysis with regression in the presence of viscous dissipation was accounted by Jahan *et al.*, [8] to re-examine a model of boundary layer flow in a preambly stretching/shrinking sheet over a moving surface. In the existence of viscous dissipation, Lund *et al.*, [9] analyzed a Casson fluid past an exponentially vertical shrinking surface together with stability analysis. The hybrid nanofluid over exponentially shrinking sheet addressed by Anuar *et al.*, [10] considered Ag nanoparticle into $Cuo/water$ nanoparticle with stability analysis.

The majority of the literature discussed earlier took into consideration the steady state situation. However, in almost all engineering application devices involve unsteadiness in their aerodynamic environments such as the rotor helicopter and the cascades of blades of turbomachinery. In unsteady flow, the fluid characteristic varies with respect to time, which affects the fluid motion and also the separation of the boundary layer. Choudhury and Drake [11] explored the features of time-dependent stagnation point flow 2-D. Sandeep and Sulochana [12] worked on the mixed convection boundary layer for the time-dependent flow of magnetic micropolar fluid through a permeable stretching surface. The features of unsteady non-Newtonian nanofluid flow over a permeable stretching wall along with the combined effects of magnetic field and heat source/sink addressed by Eid and Mahny [13].

Recently, Poulomi [14] carried out an analysis of the effect of Soret and Dufour with heat and mass transmission on an unsteady flow over a semi-infinite vertical plate. El-Kabeir *et al.*, [15] examined time-dependent Ferrofluid slip flow over an impulsively stretchable sheet with mixed convection. The unsteady hybrid nanofluid addressed by Waini *et al.*, [16] by considered Al_2O_3 and Cu as a nanoparticle in water past a stretching/shrinking surface with mass suction.

A carbon nanotube CNT_s are typical shape material in nano-size, made up of carbon, have exceptional thermal conductivity, tensile strength and optical properties. Carbon nanotubes are mainly classified into two categories i.e., single-wall carbon nanotube known as $SWCNT_s$ has only one layer and multi-wall carbon nanotube known as $MWCNT_s$, is a collection of nested tubes of continuously increasing diameter. CNT_s has a wide range of various useful applications include sensors, solar cell, smart textiles, transparent conductors, semiconductors, batteries, oscillator and microelectronic devices. Due to all these various applications, researchers are actively working on the industry evolution of CNT_s . Iijima [17] provided a new type of finite carbon structure or scrutinized carbon nanotube CNT_s in diameter size 4-30 nm. The concept of $SWCNT_s$ introduced by Iijima [18]. Hayat *et al.*, [19] numerically scrutinized the characteristics of melting heat transfer in carbon nanotube via a stretched sheet with a variable thickness. The impact of stretching/shrinking sheet and suction/injection in CNT_s was accounted by Norzawary *et al.*, [20]. Anuar *et al.*, [21] carried out the consideration of the boundary layer flow through a continuous moving sheet in carbon nanotube with stability analysis. The unsteady hybrid nanofluid addressed by Gohar *et al.*, [22] considered

$MWCNT_s$ and Al_2O_3 as nanoparticle in cementitious. Recently, Hussanan *et al.*, [23] highlighted the influence of carbon nanotube past a linearly stretching plate with the impact of thermal radiation and Newtonian heating. Based in the above discussed literacy, most of the studies examined different characteristics and properties of steady of CNT_s over various geometry. To fill the gap, the behaviors of unsteady flow and heat transfer of CNT_s accounted through flat surface.

2. Methodology Modeling

Initially, a two-dimensional unsteady stagnation point with two types of nanoparticles $SWCNT_s$ and $MWCNT_s$ are considered. The flow is laminar and incompressible. The free stream velocity (outer layer) is $U_\infty(x, t) = ax(1 - ct)^{-1}$ where a and c are positives constants it is assumed the plate temperature T_w and also ambient fluid temperature T_∞ are constants. The x -axis parallel to the flow direction and y -axis perpendicular to it. Based on the above assumption the basic governing equations in unsteady state are respectively as below:

$$\frac{\partial u}{\partial x} + \frac{\partial v}{\partial y} = 0 \tag{1}$$

$$\frac{\partial u}{\partial t} + u \frac{\partial u}{\partial x} + v \frac{\partial v}{\partial y} = \frac{\partial U_\infty}{\partial t} + U_\infty \frac{\partial U_\infty}{\partial x} + \frac{\mu_{nf}}{\rho_{nf}} \frac{\partial^2 u}{\partial y^2} \tag{2}$$

$$\frac{\partial T}{\partial t} + u \frac{\partial T}{\partial x} + v \frac{\partial T}{\partial y} = \alpha_{nf} \frac{\partial^2 T}{\partial y^2} \tag{3}$$

Note that (u, v) represents the velocity components along the Cartesian coordinates axis. While the corresponding boundary conditions are:

$$\begin{aligned} t < 0 : u = v = 0, & & T = T_\infty & \text{for any } x, y \\ t \geq 0 : u = 0, v = 0, & & T = T_w & \text{at } y = 0 \\ u \rightarrow U_\infty(x, t) & & T \rightarrow T_\infty & \text{as } y \rightarrow \infty \end{aligned} \tag{4}$$

Here, T represents the temperature, μ_{nf} the effective viscosity of nanoparticle, α_{nf} the effective thermal diffusivity of nanoparticle and ρ_{nf} is the density of the nanoparticle. Based on the Maxwell theory a theoretical model proposed by Xue [24]. To determine the distribution of CNT_s .

$$\alpha_{nf} = \frac{k_{nf}}{(\rho C_p)_{nf}}, \quad \mu_{nf} = \frac{\mu_f}{(1-\phi)^{2.5}}, \quad \rho_{nf} = (1 - \phi)\rho_{CNT}$$

$$(\rho C_p)_{nf} = (1 - \phi)(\rho C_p)_f + \phi(\rho C_p)_{CNT}$$

$$\frac{k_{nf}}{k_f} = \frac{1-\phi+2\phi \frac{k_{CNT}}{k_{CNT}-k_f} \ln \frac{k_{CNT}+k_f}{2k_f}}{1-\phi+2\phi \frac{k_f}{k_{CNT}-k_f} \ln \frac{k_{CNT}+k_f}{2k_f}} \tag{5}$$

Note that, ϕ refers to nanoparticle volume fraction, μ_f stands for the effective viscosity for the carrier fluid. The effective dynamic viscosity of nanoparticle is μ_{nf} given by Brinkman [25]. The parameter of heat capacitance of nanoparticle is denoted via $(\rho C_p)_{nf}$ the thermal conductivity for both of (carrier fluid) and (carbon nanotubes) denoted via k_f and k_{CNT} respectively. The thermal

conductivity if the nanofluid is denoted via k_{nf} . While ρ_f and ρ_{CNT} are the density of a carrier fluid and carbon nanotubes, respectively. The similarity solution is expressed as

$$\eta = \left(\frac{a}{v_f(1-ct)}\right)^{1/2} y, \quad \psi = \left(\frac{v_f a}{1-ct}\right)^{1/2} xf(\eta), \quad \theta(\eta) = \frac{T-T_\infty}{T_w-T_\infty} \quad (6)$$

Here, the stream function ψ illustrates as usual form $u = \frac{\partial\psi}{\partial y}$ and $v = -\frac{\partial\psi}{\partial x}$ which satisfied conservation of mass equation in Eq. (1). Further, using Eq. (6) to transform Eq. (2) and (3) with the initial and boundary condition from Eq. (4) to the following

$$\frac{1}{(1-\phi)^{2.5}(1-\phi+\phi\rho_{CNT}/\rho_f)} + f'''' + ff' - f'^2 + 1 - A\left(f^1 + \frac{1}{2}\eta f'' - 1\right) = 0 \quad (7)$$

$$\frac{1}{p_r} \frac{k_{nf}/k_f}{[1-\phi+\phi(\rho C_p)_s/(\rho C_p)_f]} \theta'' + \left(f - \frac{A}{2}\eta\right) \theta' = 0 \quad (8)$$

The transformed boundary conditions are

$$\begin{aligned} f(0) = 0, \quad f'(0) = 0, \quad \theta(0) = 1 \\ f'(\eta) \rightarrow 1, \quad \theta(\eta) \rightarrow 0 \quad \text{as } \eta \rightarrow \infty \end{aligned} \quad (9)$$

In the above equations, primes represent differentiation with respect to η , prandtl number defined as $p_r = \frac{v_f}{\alpha_f}$ and the unsteady parameter A is defined as $A = c/a$, where both of $a > 0$ and c are constants. It is valuable to mention that in the absence of CNT_s ($\phi = 0$) and $A = 0$ (i.e. steady state) Eq. (7) reduces to a steady 2-D stagnation point flow. The expression of real amount of main interest, such as skin friction coefficient C_f along with Nusselt number Nu_x , are respectively represented as

$$C_f = \frac{T_w}{\rho_f U_\infty^2}, \quad Nu_x = \frac{xq_w}{k_f(T_w-T_\infty)} \quad (10)$$

where T_w represent shear stress at the surface, and q_w represent heat flux from the surface can be expressed as below

$$T_w = \mu_{nf} \left(\frac{\partial u}{\partial y}\right)_{y=0}, \quad q_w = -k_{nf} \left(\frac{\partial T}{\partial y}\right)_{y=0} \quad (11)$$

With μ_{nf} represent dynamic viscosity and k_{nf} represent thermal conductivity. Using Eq. (6) we obtain

$$C_f Re_x^{1/2} = \frac{1}{(1-\phi)^{2.5}} f''(0) \quad (12)$$

$$Nu_x / Re_x^{1/2} = -\frac{k_{nf}}{k_f} \theta'(0) \quad (13)$$

where $Re_x = U_\infty x / v_f$ refers to confined Reynold number.

3. Numerical Method

In the current model, the scheme of non-linear ordinary differential equations, in Eq. (7) and (8) together with the initial and boundary condition are numerically attained through utilized *bvp4c* package in Matlab. Dual solution is observable by utilizing various initial guess equipped at an initial mesh point and to obtain precise accuracy we change the step size. The detailed of this method is given by Shampine *et al.*, [26]. It is essential in this method to reduce the scheme of ordinary differential equations to first order. The finding process for both skin friction $f''(0)$ and heat transfer coefficient $-\theta'(0)$ is keep repeated until no more solution is can be obtained beyond the critical point A_c .

4. Results and Discussions

The outcome of nanoparticle volume fraction ϕ and the unsteadiness parameter (A) are investigated and presented graphically in this section. Nanoparticle volume fraction is varying ($0 < \phi < 0.2$) where water was considered as carrier fluid with Prandtl number 6.2 ($pr = 6.2$), in which ($\phi = 0$) is corresponding to regular fluid. The thermos-physical properties of water and CNT_s are given in Table 1 provided by Khan [27].

Table 1
 Thermos-physical properties of carrier fluid and CNT_s

Physical properties	(carrier fluid)	(nanoparticle)	
	Water ($pr = 6.2$)	$SWCNT_s$	$MWCNT_s$
$\rho(kg/m^3)$	997	2600	1600
$C_p(J/kgK)$	4179	425	796
$k(W/mK)$	0.613	6600	3000

Validation of numerical procedure achieved by direct comparison between the numerical outcome of the presents work with the numerical outcome communicated previously by Backok *et al.*, [28]. When the steady state ($A = 0$) and $\phi = 0$ it is found that $f''(0) = 1.232587654$, while Backok *et al.*, [28] reported that the value $f''(0) = 1.232587669$ which deemed fascinatingly agreed. Meanwhile, Table 2 shows the value of $f''(0)$ and $-\theta'(0)$ for some specific values of A , where ($SWCNT_s, MWCNT_s$) with water ($\phi = 0.1$).

Table 2
 The values of $f''(0)$ and $-\theta'(0)$ for selected value of A

A	$SWCNT_s$ $f''(0)$	$-\theta'(0)$	$MWCNT_s$ $f''(0)$	$-\theta'(0)$
1	1.415274	0.363052	1.352752	0.354178
-1	0.871909 [-0.930403]	1.043711 [0.338652]	0.833391 [-0.889301]	1.070315 [0.338954]
-2	0.522469 [-1.598671]	1.281834 [0.902111]	0.499388 [-1.528047]	1.320192 [0.938233]
-3	0.083985 [-1.869305]	1.483234 [1.254121]	0.080275 [-1.786726]	1.531364 [1.302621]
-4	-0.543212 [-1.820662]	1.652009 [1.540325]	-0.519215 [-1.740233]	1.708671 [1.597553]

[] represent second solution.

It is noted from the Table 2 the value of $f''(0)$ for $SWCNT_s$ is higher than $MWCNT_s$, while the value of $-\theta'(0)$ for $MWCNT_s$ is higher. This is due to $SWCNT_s$ has higher viscosity. To obtain a perspective of the flow regime, the impact of the unsteadiness parameter A and nanoparticle volume fraction ϕ on

velocity and temperature distributions are present through figures and also the physical nature scrutinized in details.

Figure 1 - 4 visualize the variation with A of the reduced skin friction $f''(0)$ and the reduced heat flux $-\theta'(0)$ for some values of A and ϕ . It is noted that only one solution found for $(A > 0) \cup (A = A_c)$, here A_c is the value where the upper branch solution encounters the lower branch solution. Pair solutions, an upper and lower branch solutions for $A < A_c < 0$. No dual solution occurs beyond the critical value which is $A_c = -4.5066$, due to the boundary layer separation from the plate. Decreasing A will decrease the value of $f''(0)$ for the upper and lower branch from positive to negative values. The first solution upper branch turns out at this point goes on to the second solution lower branch. At certain value of A , the lower branch solutions end up.

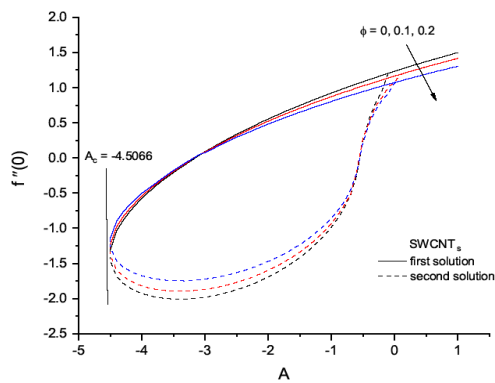


Fig. 1. impact of A on $f''(0)$ for some values of $\phi(0 < \phi < 0.2)$ for $SWCNT_s$

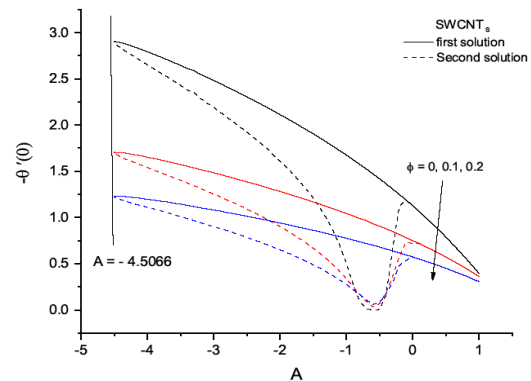


Fig. 2. Impact of A on $-\theta'(0)$ for some values of $\phi(0 < \phi < 0.2)$ for $SWCNT_s$

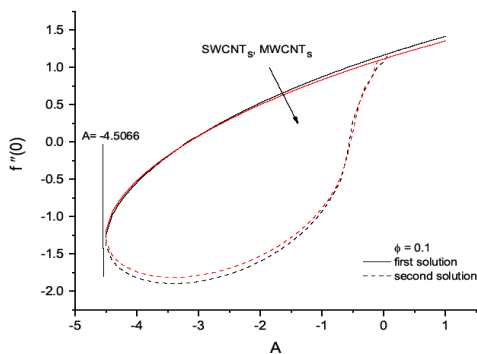


Fig. 3. Impact of A on $f''(0)$ for some values of for $SWCNT_s$ and $MWCNT_s$ when $\phi = 0.1$

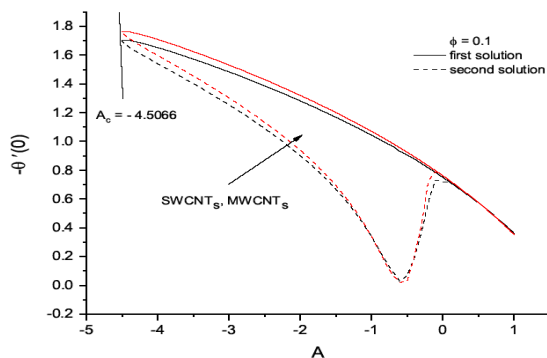


Fig. 4. Impact of A on $-\theta'(0)$ for some values of for $SWCNT_s$ and $MWCNT_s$ when $\phi = 0.1$

Figure 2 and 4 visualise the domain of solution of the temperate distribution at the surface $-\theta'(0)$, which is proportional to the local Nusselt number. The first solution (upper branch) and the second solution (lower branch) indicate the curves displayed in Figure 1- 4. It is noticed the value of the first solution for $f''(0)$ and $-\theta'(0)$ larger than second solution. It is noted that the values of an unsteadiness parameter A get increases through decreases $-\theta'(0)$. Figure 5 and 6 are plotted for the coefficient of the skin friction $C_f Re_x^{1/2}$ and local Nusselt number $Nu_x / Re_x^{1/2}$ with control volume fraction ϕ for both $SWCNT_s$ and $MWCNT_s$ when $A = -0.4$. It is seen from the figures, both of heat

transfer heat and skin friction increasing linearly. Besides this, the heat transfer rate and the skin friction for $SWCNT_s$ is higher than $MWCNT_s$ as $SWCNT_s$ has higher thermal conductivity compare with $MWCNT_s$.

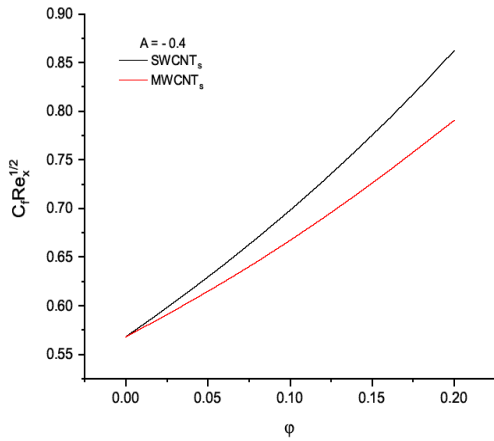


Fig. 5. Impact of ϕ on skin friction coefficient for $SWCNT_s$ and $MWCNT_s$ when $A = -0.4$

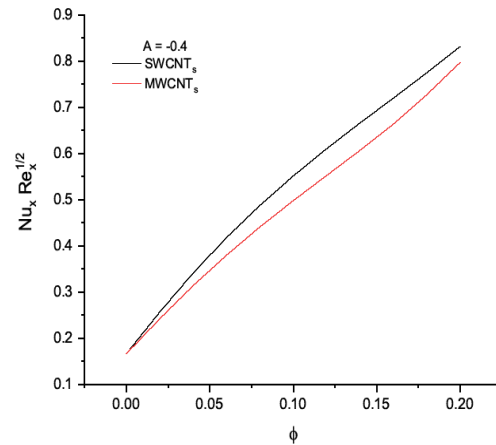


Fig. 6. Impact of ϕ on Nusselt number for $SWCNT_s$ and $MWCNT_s$ when $A = -0.4$

The velocity profile along with temperature profile are presented in Figure 7-10. These profiles are satisfied with the boundary condition in Eq. (9) asymptotically fulfilled. Which gives support the validation of the numerical outcomes and also the existence of the pair solutions. Besides this, the boundary layer thickness for the first solution is found thinner than the second solution in all cases. Figure 7 and 9 showed the converged solution when the plot of velocity profile $f'(\eta)$ approach to 1 while the thickness of the boundary layer is less than 5. Figure 8, signifies the impact of ϕ on $SWCNT_s$ while Figure 10, signifies the variation of temperature profile in both nanotubes.

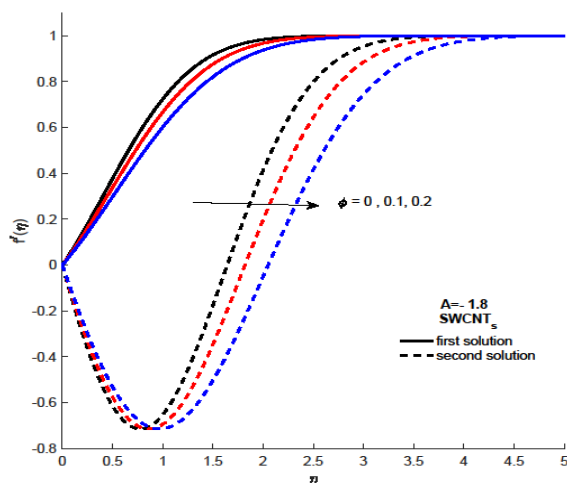


Fig. 7. Impact of ϕ on velocity profile for $SWCNT_s$

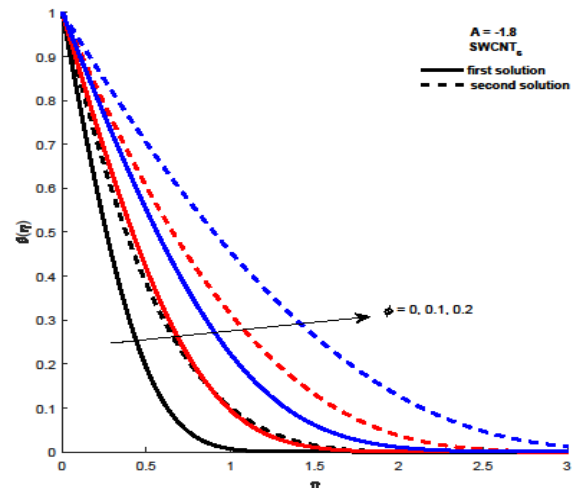


Fig. 8. Impact of ϕ on temperature profile for $SWCNT_s$

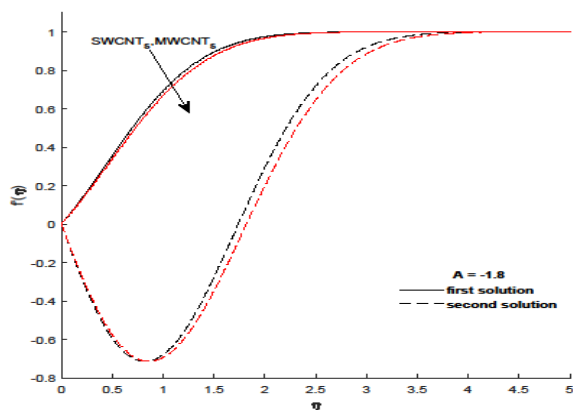


Fig. 9. Velocity profile for $SWCNT_s$ and $MWCNT_s$

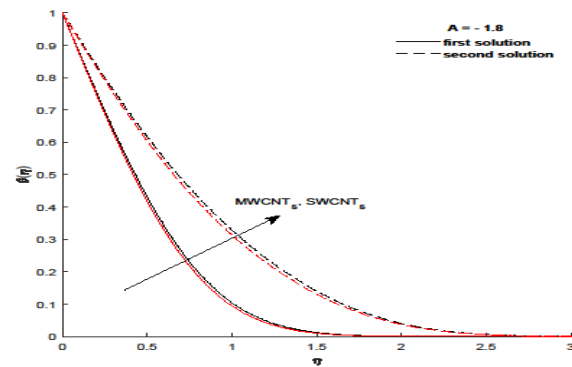


Fig. 10. Temperature profile for $SWCNT_s$ and $MWCNT_s$

5. Conclusions

Here, unsteady 2-D stagnation point flow of nanofluid comprising both nanotubes are explored. The mathematical model of nonlinear partial differential equation is converted to scheme of ordinary differential equation through using similarity method. Then, attained numerically for $SWCNT_s$ and $MWCNT_s$. The key points of our analysis can be stated as

- i. Dual solution obtained for time-dependent flow when unsteadiness parameter A is a negative value (decelerated flow).
- ii. Implement of $SWCNT_s$ and $MWCNT_s$ into carrier fluid will increase the skin friction and heat transfer coefficient.
- iii. Both of heat transfer rate as well as skin friction are higher for $SWCNT_s$ than $MWCNT_s$ at the surface.

Acknowledgement

The corresponding author is highly appreciated for the financially received from Universiti Putra Malaysia.

References

- [1] Choi, Stephen US, and Jeffrey A. Eastman. *Enhancing thermal conductivity of fluids with nanoparticles*. No. ANL/MSD/CP-84938; CONF-951135-29. Argonne National Lab., IL (United States), 1995.
- [2] Buongiorno, Jacopo. "Convective transport in nanofluids." (2006): 240-250.
<https://doi.org/10.1115/1.2150834>
- [3] Tiwari, Raj Kamal, and Manab Kumar Das. "Heat transfer augmentation in a two-sided lid-driven differentially heated square cavity utilizing nanofluids." *International Journal of heat and Mass transfer* 50, no. 9-10 (2007): 2002-2018.
<https://doi.org/10.1016/j.ijheatmasstransfer.2006.09.034>
- [4] Bachok, Norfifah, Anuar Ishak, Roslinda Nazar, and Norazak Senu. "Stagnation-point flow over a permeable stretching/shrinking sheet in a copper-water nanofluid." *Boundary Value Problems* 2013, no. 1 (2013): 39.
<https://doi.org/10.1186/1687-2770-2013-39>
- [5] Das, M., B. K. Mahatha, and R. Nandkeolyar. "Mixed convection and nonlinear radiation in the stagnation point nanofluid flow towards a stretching sheet with homogenous-heterogeneous reactions effects." *Procedia Engineering* 127 (2015): 1018-1025.
<https://doi.org/10.1016/j.proeng.2015.11.451>
- [6] Uddin, Md Jashim, W. A. Khan, and Ahmad Izani Md Ismail. "Similarity solution of double diffusive free convective flow over a moving vertical flat plate with convective boundary condition." *Ain Shams Engineering Journal* 6, no. 3 (2015): 1105-1112.

- <https://doi.org/10.1016/j.asej.2015.01.008>
- [7] Ahmad, Kartini, and Anuar Ishak. "Magnetohydrodynamic (MHD) Jeffrey fluid over a stretching vertical surface in a porous medium." *Propulsion and Power Research* 6, no. 4 (2017): 269-276.
<https://doi.org/10.1016/j.jprr.2017.11.007>
- [8] Jahan, Shah, Hamzah Sakidin, Roslinda Nazar, and Ioan Pop. "Analysis of heat transfer in nanofluid past a convectively heated permeable stretching/shrinking sheet with regression and stability analyses." *Results in Physics* 10 (2018): 395-405.
<https://doi.org/10.1016/j.rinp.2018.06.021>
- [9] Lund, Liaquat Ali, Zurni Omar, and Ilyas Khan. "Steady incompressible magnetohydrodynamics Casson boundary layer flow past a permeable vertical and exponentially shrinking sheet: A stability analysis." *Heat Transfer—Asian Research* 48, no. 8 (2019): 3538-3556.
<https://doi.org/10.1002/htj.21554>
- [10] Anuar, Nur Syazana, Norfifah Bachok, Norihan Md Arifin, and Haliza Rosali. "Effect of Suction/Injection on Stagnation Point Flow of Hybrid Nanofluid over an Exponentially Shrinking Sheet with Stability Analysis." *CFD Letters* 11, no. 12 (2019): 21-33.
- [11] Choudhury, P. N., and D. G. Drake. "Unsteady stagnation point flow." *Applied Scientific Research* 25, no. 1 (1972): 193-200.
<https://doi.org/10.1007/BF00382295>
- [12] Sandeep, N., and C. Sulochana. "Dual solutions for unsteady mixed convection flow of MHD micropolar fluid over a stretching/shrinking sheet with non-uniform heat source/sink." *Engineering Science and Technology, an International Journal* 18, no. 4 (2015): 738-745.
<https://doi.org/10.1016/j.jestch.2015.05.006>
- [13] Eid, Mohamed R., and Kasseb L. Mahny. "Unsteady MHD heat and mass transfer of a non-Newtonian nanofluid flow of a two-phase model over a permeable stretching wall with heat generation/absorption." *Advanced Powder Technology* 28, no. 11 (2017): 3063-3073.
<https://doi.org/10.1016/j.appt.2017.09.021>
- [14] De, Poulomi. "Soret-Dufour Effects on Unsteady Flow of Convective Eyring-Powell Magneto Nanofluids over a Semi-Infinite Vertical Plate." *BioNanoScience* 9, no. 1 (2019): 7-12.
<https://doi.org/10.1007/s12668-018-0583-7>
- [15] El-Kabeir, S. M. M., E. R. El-Zahar, Mohammed Modather, R. S. R. Gorla, and A. M. Rashad. "Unsteady MHD slip flow of a ferrofluid over an impulsively stretched vertical surface." *AIP Advances* 9, no. 4 (2019): 045112.
<https://doi.org/10.1063/1.5088610>
- [16] Waini, Iskandar, Anuar Ishak, and Ioan Pop. "Unsteady flow and heat transfer past a stretching/shrinking sheet in a hybrid nanofluid." *International Journal of Heat and Mass Transfer* 136 (2019): 288-297.
<https://doi.org/10.1016/j.ijheatmasstransfer.2019.02.101>
- [17] Iijima, Sumio. "Helical microtubules of graphitic carbon." *nature* 354, no. 6348 (1991): 56-58.
<https://doi.org/10.1038/354056a0>
- [18] Iijima, Sumio, and Toshinari Ichihashi. "Single-shell carbon nanotubes of 1-nm diameter." *nature* 363, no. 6430 (1993): 603-605.
<https://doi.org/10.1038/363603a0>
- [19] Hayat, T., Khursheed Muhammad, M. Farooq, and A. Alsaedi. "Melting heat transfer in stagnation point flow of carbon nanotubes towards variable thickness surface." *AIP advances* 6, no. 1 (2016): 015214.
<https://doi.org/10.1063/1.4940932>
- [20] Norzawary, Nur Hazirah Adilla, Norfifah Bachok, and Fadzilah Md Ali. "Stagnation Point Flow over a Stretching/shrinking Sheet in a Carbon Nanotubes with Suction/Injection Effects." *CFD Letters* 12, no. 2 (2020): 106-114.
- [21] Anuar, Nur Syazana, Norfifah Bachok, and Ioan Pop. "A stability analysis of solutions in boundary layer flow and heat transfer of carbon nanotubes over a moving plate with slip effect." *Energies* 11, no. 12 (2018): 3243.
<https://doi.org/10.3390/en11123243>
- [22] Gohar, Madeha, Farhad Ali, Ilyas Khan, Nadeem Ahmad Sheikh, and Attaullah Shah. "The unsteady flow of generalized hybrid nanofluids: applications in cementitious materials." *Journal of the Australian Ceramic Society* 55, no. 3 (2019): 657-666.
<https://doi.org/10.1007/s41779-018-0275-3>
- [23] Hussanan, Abid, Ilyas Khan, Mohammad Rahimi Gorji, and Waqar A. Khan. "CNT S-Water-Based Nanofluid Over a Stretching Sheet." *BioNanoScience* 9, no. 1 (2019): 21-29.
<https://doi.org/10.1007/s12668-018-0592-6>

-
- [24] Xue, Q. Z. "Model for thermal conductivity of carbon nanotube-based composites." *Physica B: Condensed Matter* 368, no. 1-4 (2005): 302-307.
<https://doi.org/10.1016/j.physb.2005.07.024>
- [25] Brinkman, H. C. "The viscosity of concentrated suspensions and solutions." *The Journal of Chemical Physics* 20, no. 4 (1952): 571-571.
<https://doi.org/10.1063/1.1700493>
- [26] Shampine, Lawrence F., Ian Gladwell, Larry Shampine, and S. Thompson. *Solving ODEs with matlab*. Cambridge university press, 2003.
<https://doi.org/10.1017/CBO9780511615542>
- [27] Khan, W. A., Z. H. Khan, and M. Rahi. "Fluid flow and heat transfer of carbon nanotubes along a flat plate with Navier slip boundary." *Applied Nanoscience* 4, no. 5 (2014): 633-641.
<https://doi.org/10.1007/s13204-013-0242-9>
- [28] Bachok, Norfifah, Anuar Ishak, and Ioan Pop. "The boundary layers of an unsteady stagnation-point flow in a nanofluid." *International Journal of Heat and Mass Transfer* 55, no. 23-24 (2012): 6499-6505.
<https://doi.org/10.1016/j.ijheatmasstransfer.2012.06.050>